Molecular Orientation of Blue Luminescent Rigid−Flexible Polymers

V. Deimede,[†,‡] K. S. Andrikopoulos,[†,§] G. A. Voyiatzis,*[,†] F. Konstandakopoulou,[‡] and J. K. Kallitsis[†,‡]

Foundation for Research & Technology-Hellas (FORTH), Institute of Chemical Engineering and High-Temperature Chemical Processes (ICE/HT), P.O. Box 1414, GR-265 00 Patras, Greece, Department of Chemistry, University of Patras, GR-265 00 Patras, Greece, and Department of Chemical Engineering, University of Patras, GR-265 00 Patras, Greece

Received July 8, 1999; Revised Manuscript Received October 21, 1999

ABSTRACT: Polymeric films of rigid−flexible luminescent polyethers containing substituted quinquephenyl units in the main chain and films of their diluted blends in polypropylene have been uniaxially drawn at temperatures above their glass transition. Polarized micro-Raman measurements have been conducted to evaluate the molecular orientation of the drawn polymers and probe the effect of side chain length and type. The second, P_2, and fourth, P_4, moments of the segmental orientation distribution function determined from the analysis of Raman spectra indicate that the longer the side-chain length is, the higher the molecular orientation attained. At short side chain lengths, the presence of an oxygen link between the alkyl side chain and the aromatic segment resulted in a restricted polymer orientation. Polarized photoluminescence measurements have shown that neat photonic polyethers display low dichroic ratios despite the high orientability shown in Raman measurements. Diluted blends of photonic polyethers in polypropylene have shown commensurate high orientation moments in Raman and enhanced dichroic ratio in photoluminescence. The implication on the perspective of the studied polyethers to give materials with polarized blue light emission is evident.

Introduction

Molecular orientation in polymers is of great technical and theoretical importance for controlling processing and tailoring the physical properties of the final product.[1,2] In the past few decades, a lot of progress has been made in the development of methodologies for studying and accurately evaluating this important property.[1−11] Orientation in polymers can be accomplished by film stretching,[12−14] deposition on oriented substrates,[15−19] or the liquid crystallinity approach.[20−22]

Polarized Raman spectroscopy has been proved a valuable tool for molecular orientation evaluation, since it provides independent information on both the second ($\langle P_2(\cos\theta)\rangle = [3\langle\cos^2\theta\rangle - 1]/2$, with θ being the orientation angle) and the fourth ($\langle P_4(\cos\theta)\rangle = [35\langle\cos^4\theta\rangle - 30\langle\cos^2\theta\rangle + 3]/8$) moments of the expansion of the orientation distribution function.[23−26]

This paper concentrates on the molecular orientation of conjugated polymers, an exciting class of materials with a wide range of optical and electrical properties.[27] From scientific as well as practical point of view, it is important to establish the molecular architecture[28] needed to ensure specific chain configuration and develop techniques[12,20,29] to provide control over the structure, orientation, and molecular organization of these materials, since they are candidates for polarized light emission. In fact, the introduction of uniaxial molecular orientation into films of conjugated luminescent polymers was naturally found to yield structures that emit polarized light. The use of highly linear polarized layers in the design of LC-based photoluminescent display devices has been recently reported.[30] Orientation evaluation provides a basis for establishing molecular mechanisms of deformation and may still contribute to a better understanding of the interrelationship between technological properties and polymer structure.

In conjugated polymers, the strategy, based on the synthesis of copolymers bearing defined conjugated segments linked by a flexible spacer, has been proven useful to control the conjugation length, to improve processability, and to result in materials with good mechanical properties. Conjugated segments such as phenylene−vinylene,[31] oligothiophene,[32] oligophenylene,[33,34] and bis(styryl)anthracene[35] have been introduced in rigid−flexible polymers. Some of these polymers show improved mechanical properties[34,35] and can be oriented by uniaxial stretching at temperatures above their glass transition. The improvements on mechanical and luminescent properties resulting from chain extension, chain alignment, and structural order are general phenomena, and in principle, photonic excitation of uniaxially stretched films of this class of polymers should result in linear polarized light emission.

Aromatic−aliphatic polyethers containing alkyl- or alkyloxy-substituted quinquephenyl units have been recently synthesized[34] and found to combine solubility and film-forming properties with liquid crystalline behavior at temperatures where the polymers are thermally stable. Moreover, these polyethers exhibit blue-light emission,[34] a photophysical property that, when combined with orientation at the molecular level, seems to be a promising concept for new optical materials. This is precisely the scope of this paper, to investigate the molecular orientation of such aromatic−aliphatic uniaxially drawn polyether films, bearing alkyl or alkyloxy side chains of different sizes, at different draw ratios. To achieve that, we have utilized laser Raman microscopy. The analysis of Raman scattering has been already extensively applied in polymers to get information on their molecular orientation[26,36−38] and

[†] Institute of Chemical Engineering and High-Temperature Chemical Processes.
[‡] Department of Chemistry, University of Patras.
[§] Department of Chemical Engineering, University of Patras.

10.1021/ma9911041 CCC: $18.00
Published on Web 12/03/1999

Chart 1. Molecular Structure of PETH−Ph5/S.R Model Polyethers[a]

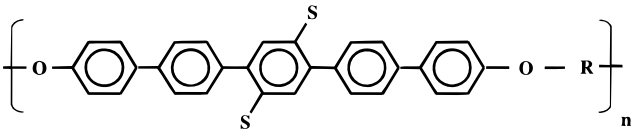

[a] S = C_6H_{13}, OC_6H_{13}, or $OC_{12}H_{25}$; R = C_7H_{14} , C_9H_{18}, $C_{10}H_{20}$, or $C_{11}H_{22}$. (n = number of repeat units.)

to the study of polyconjugated aromatic materials with electrical and nonlinear optical properties.[39] Likewise, vibrational spectroscopy has been recently used in the investigation of the effects of the side chain length on the orientability of uniaxially drawn hairy-rod model polyesters.[38] These results have demonstrated the ability of polarized Raman microscopy to evaluate the molecular orientation of the polyester films and, moreover, to resolve the size of the side chain that enhances the processing performance of these materials. This represents a motivation also for the present work, to probe by Raman microscopy the effect of the substituents as well as of the flexible spacer length on the orientability of these rigid−flexible polyether films. In this paper, polarized photoluminescence measurements using either diffused or polarized excitation light have been also conducted on a representative polyether film drawn as neat polymer as well as diluted blend in isotactic polypropylene. This photophysical investigation tried to correlate the anticipated polarized light emission with the molecular orientation evaluated by micro-Raman spectroscopy.

Experimental Section

Materials. Model polyethers [PETH] with the chain backbone consisting of an aromatic (Ar) rigid rod and an aliphatic (C_nH_{2n}, R) flexible spacer [PETH−Ar.R] were utilized. The synthesis of the aromatic aliphatic polyethers containing substituted (S) quinquephenyl (Ph5) segments [PETH−Ph5/S.R] has been published elsewhere;[34] substituents of hexyl [PETH−Ph5/C6.R], hexyloxy [PETH−Ph5/OC6.R], and dodecyloxy [PETH−Ph5/OC12.R] side chains have been used. The aliphatic flexible spacer length varied between 7 and 11 methylene units. The generalized polymer structure is schematically shown in Chart 1.

In all cases, self-supported films were obtained by melt pressing in a temperature range of 200−250 °C, depending on the polymer structure. Uniaxially oriented films were obtained by drawing the films in a thermostated chamber at temperatures 20−30 °C above their glass transition temperatures. The standard drawing speed was ca. 2 cm/min, and the dimensions of the specimen were 2 cm in length, 0.3 cm in width, and 0.01 cm in thickness. In most cases, draw ratios between 1.5 and 5.0 have been achieved for the homopolymers.

Blends were prepared by casting a solution of the photonic polymer (2.5 or 5 mg) and the polypropylene (isotactic, Ega-Chemie) in xylene (50 mL) dissolved by heating at 130 °C. The resulting films were dried under vacuum at 60 °C for 24 h and melt pressed at 220 °C. Draw ratios of 2.0 to 10.0 have been obtained by drawing the films at 100 °C. Speed drawing and sample dimensions were the same as those for the neat polyethers.

Laser Raman Microscopy. The T-64000 micro-Raman system from Jobin Yvon (ISA-Horiba group) was used. Raman spectra were excited by a linearly polarized monochromatic radiation at 514.5 nm produced by a Spectra Physics air-cooled Ar^+ laser (model 163-A42). A proper interference filter rejected plasma lines. Excitation beam was directed toward the microscope and with the use of a beam splitter and a microscope objective (50×/0.55 Olympus) it was focused onto the sample. Raman-scattered radiation was collected in backscattering geometry by the same microscope objective and passing through the beam splitter and a notch filter was focused on the slit of a single monochromator. The dispersion and the detection were done by a 1800-grooves/mm grating and by a 2D CCD detector (operating at 140 K), respectively. The resolution capability was kept at approximately 7 cm^{-1}.

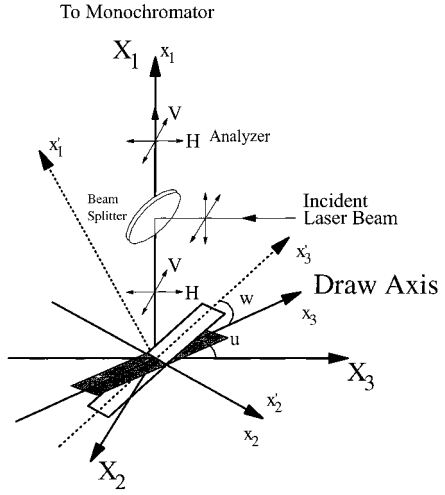

Figure 1. Coordinate axes for backscattering Raman geometry (see text for details).

The incident beam polarization was selected by an optical rotator (90°). The scattered radiation was analyzed by a dichroic sheet polarizer, and a half-wave plate was used after it whenever needed in order to ensure the same (maximum) polarization response from the grating. All spectra were corrected by taking into account the beam splitter's response to polarization of incident and scattered radiation. The total response of the system was checked using CCl_4 as a reference sample.

The backscattering geometry used to deduce the orientational moments of the uniaxially stretched aromatic aliphatic polyethers containing substituted quinquephenyl segments is depicted in Figure 1. Two sets of coordinate axes are fixed, one referred to the sample, $Ox_1x_2x_3$ (or $Ox_1'x_2'x_3'$, when the sample is tilted by an angle w), and the second one to the experimental setup and the laboratory, $OX_1X_2X_3$. The notation of a Raman polarization measurement comprises a combination of three letters, e.g., *h*-VV. The first small letter in italics, such as *h*, *v*, *d* or *s*, denotes the orientation of the draw axis, Ox_3 ($w = 0°$) or Ox_3' ($w \neq 0°$), relative to the laboratory fixed coordinates, $OX_1X_2X_3$: *h*, when aligned along the OX_3 axis ($u = 0°$ and $w = 0°$), *v*, when aligned along the OX_2 axis ($u = 90°$ and $w = 0°$), *d*, when aligned at the bisector of the X_3OX_2 angle ($u = 45°$and $w = 0°$), and *s*, when aligned along the OX_1 axis ($w = 90°$). The remaining two capital letters, such as HH, HV, VV, or VH, denote in each case the polarization direction of the excitation and scattered light respectively: H, when the polarization is parallel to the OX_3 axis and V, when the polarization is parallel to the OX_2 axis.

Photoluminescence. Polarized photoluminescence measurements were obtained (a) on a SPEX Fluorolog(Model F212, Spex USA) double monochromator, using polarized light (λ_o = 350 nm) for excitation and a Glan Thomson polarizer on the detector (PMT R928, Hamamatsu Japan), and (b) on a single spectrograph (T-64000 with a low dispersion grating of 600 grooves/mm) equipped with a 2D CCD detector using the diffused light of an UV lamp for excitation and a Glan-Thomson polarizer on the collection side of the back-emitted light in front of the entrance slit of the spectrograph. When an UV lamp is used, in the corresponding polarization notation, *U* denotes the excitation by diffused light.

Results and Discussion

A. Raman Measurements. In Figure 2 typical polarized micro-Raman spectra from the PETH−Ph5/

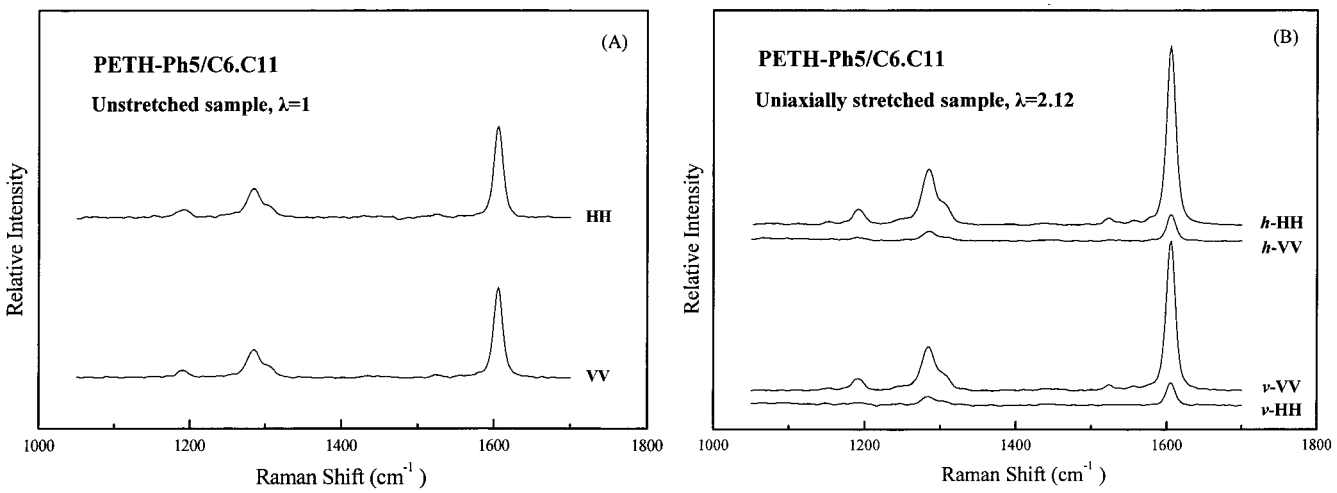

Figure 2. Polarized Raman spectra of PETH−Ph5/C6.C11 polyether films before (A) and after (B) uniaxial drawing (with draw ratio $\lambda = 2.12$), in two different polarization geometries, VV and HH, with respect to the position of the specimen, *v* or *h*, relative to the laboratory-fixed coordinates. The polarization ratio reflects the molecular orientation of the polyether. The spectra are shifted along the intensity axis for clarity.

C6.C11 samples are shown, before and after uniaxial drawing, in two different polarization geometries. It is clear that before drawing there is no preferred orientation, since the sample is essentially isotropic at molecular level; thus, there is no difference between VV and HH scattering intensities regardless of the position/orientation of the sample. In contrast, when the sample is uniaxially stretched, e.g., at a draw ratio of $\lambda = 2.12$, there are differences between relative scattering intensities in the VV and HH polarization, depending on the orientation of the draw axis of the sample with respect to the laboratory-fixed coordinates. This difference reflects the molecular orientation of the polyether, which is induced by the drawing process. For this polyether with stiff quinquephenyl unit, it is more apparent at the Raman band of the para-disubstituted phenyl ring vibration, situated at 1605 cm^{-1}. The band intensity of this C_1-C_4 skeletal phenyl ring symmetric stretch is highly enhanced in the parallel to the draw axis, and hence to the direction that the polymer backbone tends to orient, polarization geometry, *h*-HH, giving an increased polarization ratio, $I_{h-HH}/I_{h-VV} > 1$.

In Figure 3, grouped *h*-HH, *h*-HV, and *h*-VV denoted polarized Raman spectra are shown of three polyether films uniaxially stretched at the same draw ratio, $\lambda = 3$. These films bearing stiff quinquephenyl units with side chain substitution of different lengths and types contain spacer of the same length of 11 methylene groups. The spectra with polarization geometry parallel to the drawing direction, *h*-HH, have been normalized via the Raman peak intensity at 1605 cm^{-1}. In the corresponding Raman spectra of combined, *h*-HV, and crossed, *h*-VV, polarization geometries, we can clearly observe that when the flexible side chain type and length are changed, the intensity of the 1605 cm^{-1} vibrational band decreases from hexyloxy to hexyl and dodecyloxy, implying a pro rata molecular orientation increase. This is a first qualitative assessment of the effects of side chain type and length on the orientability of the polyether films. We may also notice that the Raman band at 1290 cm^{-1} assigned to the ether bond in the main chain and that at 1310 cm^{-1} due to the ether linkage in the side chain are also sensitive to the orientation. There is an increase in the polarization ratio going from hexyloxy to hexyl and dodecyloxy for the

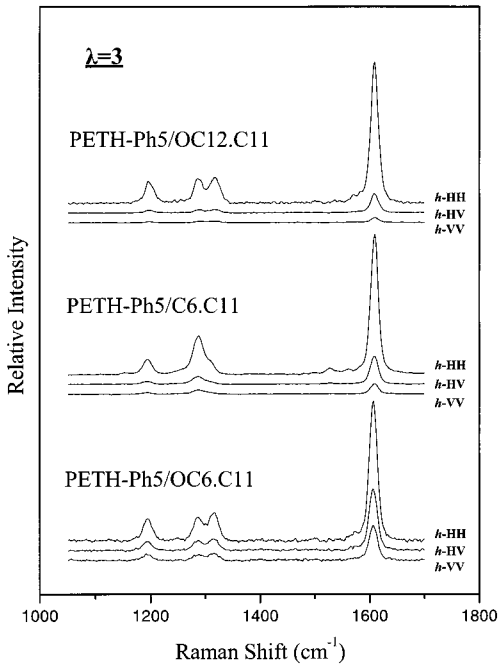

Figure 3. Grouped *h*-HH, *h*-HV, and *h*-VV polarized Raman spectra of polyether PETH−P5/OC12.C11, PETH−Ph5/C6.C11, and PETH−Ph5/OC6.C11 films uniaxially drawn at the same draw ratio, $\lambda = 3$. It is the first assessment of the effect of side chain length and type on the orientability of polyether films bearing spacer of the same length. The spectra are shifted along the vertical axis to avoid overlapping.

Raman band at 1290 cm^{-1} and from hexyloxy to dodecyloxy for the 1310 cm^{-1} band. The latter observation, concerning the ether linkage orientation of the side chain, provides a clear indication that the longer the side chain length the more it is stretched out parallel to the main chain axis promoting the molecular orientation of the corresponding polyether film.

The above finding is further confirmed in Figure 4, where the I_{h-HH}/I_{h-VV} polarization ratios for the 1605 cm^{-1} Raman band of the three uniaxially stretched polyether films (PETH−Ph5/OC6.C11, PETH−Ph5/C6.C11, PETH−Ph5/OC12.C11) are shown as a function of the draw ratio for the whole draw ratio range. These observations suggest a higher molecular orientation for

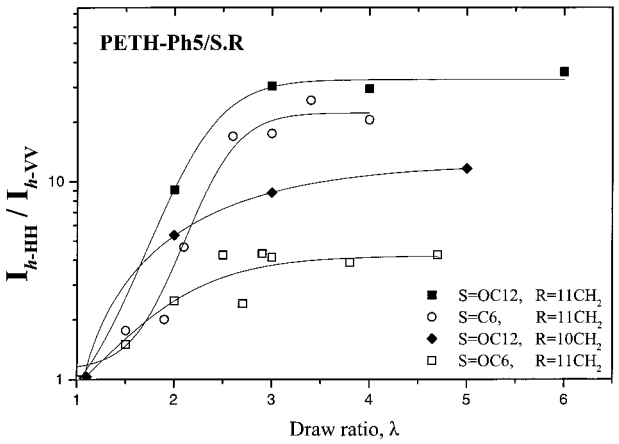

Figure 4. Polarization ratio, *h*-HH/*h*-VV, of polyether PETH−P5/OC12.C11, PETH−Ph5/C6.C11, PETH−Ph5/OC12.C10 and PETH−Ph5/OC6.C11 films for the 1605 cm^{-1} phenyl ring band, as a function of the draw ratio, for uniaxial stretching. Lines are drawn to guide the eye.

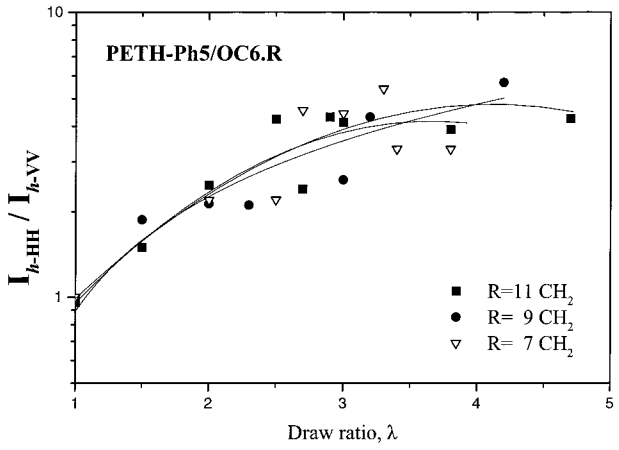

Figure 5. Polarization ratio, *h*-HH/*h*-VV, of polyether PETH−P5/OC6.C11, PETH−Ph5/OC6.C9 and PETH−Ph5/OC6.C7 films for the 1605 cm^{-1} phenyl ring band, as a function of the draw ratio, for uniaxial stretching. Lines are drawn to guide the eye.

a polyether film with longer side chains and/or absence of oxygen links between the alkyl side chain and the aromatic segment. Since the crystallinity of the samples can influence their orientational behavior, it should be noted that the sample with hexyloxy substituents, which seems to be less orientable, has lower crystallinity than that with dodecyloxy substituents.[34]

In Figure 4, additional results for the PETH−Ph5/OC12.C10 sample with a spacer of 10 methylene units are shown as well; this polyether film exhibits a lower I_{h-HH}/I_{h-VV} polarization ratio than the corresponding one with a spacer of 11 methylene units, pointing to a smaller orientation attained. This could be due to the different chain configuration resulting from the different parity in the number of methylene units.

In the same context, pertaining to the influence of the spacer length on the orientability of polyether films, the I_{h-HH}/I_{h-VV} polarization ratio for the PETH−Ph5/OC6.C*n* type film is depicted in Figure 5 bearing an odd number of methylene groups as spacers. It is noteworthy that all films of polymers bearing spacers with odd CH_2 number ($n = 7, 9, 11$), exhibit a rather similar orientation. The crystallinity of these samples vary from a $\Delta H = 10$ J/g in the sample with 11 methylene units to less than 3 J/g in the samples with nine and seven methylene units without any influence on their orientational behavior. A more systematic study on the influence of the spacer length and/or parity of methylene groups on the orientability of these rigid−flexible polyether films will be the task of further work.

B. Analysis of Raman Spectra. To deduce P_2 and P_4 for uniaxially stretched aromatic aliphatic polyethers containing substituted quinquephenyl segments, the backscattering geometry depicted in Figure 1 was used. We have adopted the analysis of Pigeon et al.,[36] based on the theory of Bower,[40] for the determination of the distribution of molecular orientation in oriented polymers from their Raman spectra. The total Raman scattering intensity is given by

$$I_s = I_o \sum (\sum I_i I_j' a_{ij})^2 \quad (1)$$

I_i and I_j' are the polarization direction of the incident and scattered light with respect to the set of axes fixed in the sample.

The experimental values are of the form $I_o \sum a_{ij} a_{pq}$, and in the case of uniaxial statistical symmetry with no preferred orientation one can write the following:

$$\sum a_{ij} a_{pq} = 4\pi^2 N_o \sum M_{l00} A_{l00}^{ijpq} \quad (2)$$

M_{l00} is expressed in terms of Legendre polynomials: $M_{l00} = (1/4\pi^2)\{(2\lambda + 1)/2\}^{1/2} \langle P_l(\cos\theta)\rangle$ ($l = 0, 2, 4$). A_{l00}^{ijpq} is a sum containing a_1, a_2, and a_3. There are only five independent nonzero sums $\sum a_{ij} \sum a_{pq}$ that are of the form $\sum a_{ii} a_{jj}$ and $\sum a_{ij}^2$, in agreement with the analysis of Mead.[41] These are as follows:

$$\sum a_{22}^2 = xR_1 + yR_2 + 3zR_3 = I_{h-VV}(w = 0°, u = 0°) \quad (3a)$$

$$\sum a_{33}^2 = xR_1 - 2yR_2 + 8zR_3 = I_{h-HH}(w = 0°, u = 0°) \quad (3b)$$

$$\sum a_{32}^2 = xR_4 - yR_5 - 4zR_3 = I_{h-VV}(w = 0°, u = 0°) \quad (3c)$$

$$\sum a_{22} a_{33} = xR_6 - yR_7 - 4zR_3 = \frac{I_{h-VV}(w = 0°, u = 0°)}{2} + \frac{I_{h-HH}(w = 0°, u = 0°)}{2} - 2I_{d-HV}(w = 0°, u = 45°) \quad (3d)$$

$$\sum a_{12}^2 = xR_4 + 2yR_5 + zR_3 = I_{s-HV}(w = 90°) \quad (3e)$$

Each nonzero sum is correlated to a specific polarization geometry (or combination of geometries) as has been already designated in the Experimental Section.

We note I_{ij} as the experimentally observed intensity of the scattered light, when the incident light is polarized parallel to the *i* axis and the scattered light is polarized parallel to the *j* axis, fixed to the laboratory. R_i are second-order polynomials of $a = a_1/a_3 = a_2/a_3$ (on the basis of literature evidence, in particular for the C_1-C_4 aromatic vibrational band at 1605 cm^{-1}, we assume that we have symmetric and cylindrical Raman tensor, i.e., the elements a_1 and a_2 of the diagonalized Raman tensor are equal),[24,26,38] $x = b$ (an experimental constant including the a_3 element of the diagonalized Raman tensor), $y = \langle P_2(\cos\theta)\rangle/b$, and $z = \langle P_l(\cos\theta)\rangle/b$.

In the above equations, parts a−e of eq 3, there are four unknowns, α, *x*, *y*, and *z*. We have to use four of

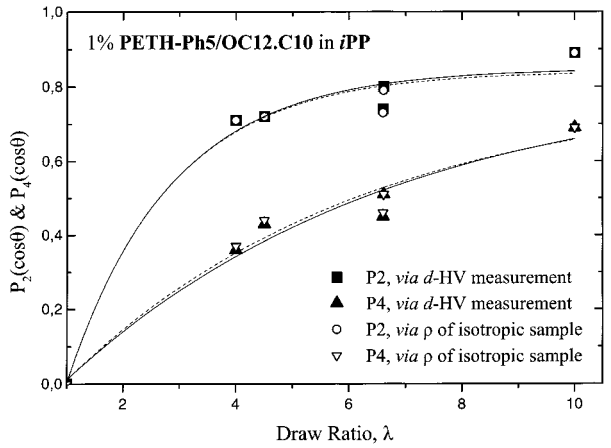

Figure 6. Second, P_2, and fourth, P_4, moments of the orientation distribution function of polyether PETH−Ph5/OC12.C10 diluted in polypropylene for the 1605 cm^{-1} phenyl ring Raman band as a function of the draw ratio. To evaluate the molecular orientation, we have considered either the polarization measurement related to eq 3d (solid symbols) or the depolarization ratio (open symbols) of an isotropic film (see text for details). Lines are drawn to guide the eye.

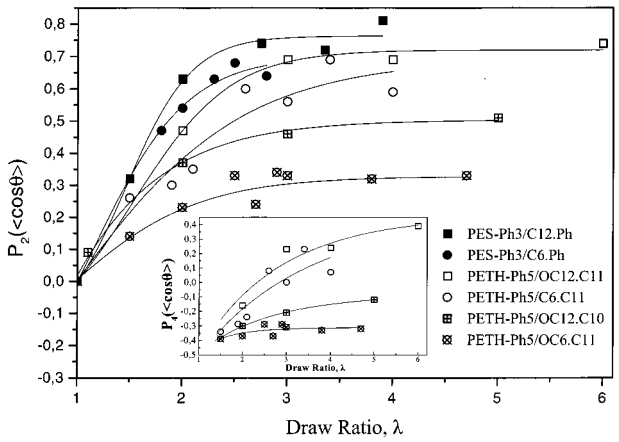

Figure 7. Second moment, P_2, of the orientation distribution function of polyether films PETH−P5/OC12.C11, PETH−Ph5/C6.C11, PETH−Ph5/OC12.C10, and PETH−Ph5/OC6.C11 from Raman measurements as a function of the draw ratio. The second moment, P_2, of the polyester films PES−Ph3/C12.Ph and PES−Ph3/C6.Ph from previous Raman measurements[38] are also included for comparison. Inset: Fourth moments, P_4, of the orientation distribution function of corresponding polyether films from Raman measurements as a function of the draw ratio. Lines are drawn to guide the eye.

the equations in order to solve the system. Equation 3e cannot be used because the polyether films are practically two-dimensional. Thus, there is no way of getting a Raman signal from that geometry; as a result, there are four remaining equations with four unknowns that form a linear algebraic system that is easy to solve analytically.

In the case of the homopolyether drawn films examined until now, the polarization measurement related to eq 3d is affected by birefringence effects of our samples. To get rid of that, we have calculated α by measuring experimentally the isotropic depolarization ratio $\rho = I_{HV}/I_{VV}$ of an isotropic (unstretched) film of the polyether diluted in PP. From the definition of the isotropic depolarization ratio, $\rho = (1 + \alpha^2 - 2\alpha)/(3 + 8\alpha^2 + 4\alpha)$, we can directly calculate α (in the hypothesis of the cylindrical Raman tensor) by measuring experimentally ρ. Calculating α we then need three equations, parts a−c of eq 3, which form a linear algebraic system, to determine the rest of the unknowns. This system has easily been solved analytically.

In drawn films of diluted blends of polyethers in isotactic polypropylene (*i*-PP), which are examined in the following sections, we deduced the second and fourth terms, $\langle P_2(\cos\theta)\rangle$ and $\langle P_4(\cos\theta)\rangle$, respectively, of the expansion of the orientation distribution function considering (a) the depolarization ratio of an isotropic film and (b) the polarization measurement related to eq 3d. In Figure 6, the second, P_2, and fourth, P_4, moments deduced from polarized Raman measurements of PETH−Ph5/OC12.C10 polyether diluted in polypropylene are shown as a function of the draw ratio. Here, we have considered either the polarization measurement related to eq 3d (solid symbols) or the depolarization ratio (open symbols) of an isotropic film. In both cases, the results obtained are almost identical accounting for negligible birefringence effect for these polymeric films.

C. Molecular Orientation and the Effect of Chain Substituents and Flexible Spacer Length. The results presented in section A have shown that there is certainly an influence of the side chain type on the orientability of PETH−Ph5/(O)C*x*.C*n* rigid−flexible polyethers. The compiled orientation data obtained for four types of polyether films bearing different side chains or/and different aliphatic spacer length are presented in Figure 7. In the same figure, the orientation data of the PES−Ph3/C*n*.Ph type ($n = 6$, 12) model polyesters are also shown. These polyesters can be directly compared with present polyethers since they exhibit the same kind of substituents at the oligophenylene moieties and instead of the flexible spacer a rigid terephthaloyl unit is present. Very recently, the analysis of polarized micro-Raman measurements on these PES−Ph3/C*n*.Ph type hairy-rod polyesters have clearly shown[38] that the polyester with longer (dodecyl, $n = 12$) side chains exhibit higher molecular orientation compared to the one with shorter (hexyl, $n = 6$) side chains.

On the basis of the results depicted in Figure 7, it is clear that PETH−Ph5/(O)C*x*.C11 type polyethers with dodecyloxy (OC12) side chain are more orientable than the corresponding ones with hexyl (C6) and particularly those with hexyloxy (OC6) substitution, although all three polyether films bear the same spacer length. As already mentioned,[34] the crystallinity of the sample with hexyl side chains is very low while the polyether with dodecyloxy side chains has the higher crystallinity supporting the view that there is no effect on the orientation caused by the crystallinity of the polymers. The differences in the orientation parameters P_2 of more than 0.4 in the PETH−Ph5/OC12.C11 and PETH−Ph5/OC6.C11 polyether films (in the plateau region) are clearly an effect of the side chain length. However, the corresponding difference in P_2 between hexyl and hexyloxy substituted polyethers is as high as 0.3 showing that the length of the side chain is not the only factor which contributes to the orientational behavior. The difference in P_2 between dodexyloxy and hexyl is only 0.1 and almost the same as previously found in PES−Ph3/C*n*.Ph hairy-rod polyesters when the side chain length was increased from hexyl ($n = 6$) to dodecyl ($n = 12$). The corresponding P_4 values that are shown in the inset of Figure 7 versus draw ratio, exhibit similar to P_2 trends, which follow the qualitative tendencies suggested by Figure 4. It is noted that the negative values P_4 can be explained as in ref 42; i.e., they correspond to

a distribution of C_1-C_4 vibrations in which all chain axes lie on a cone of angle α such that $P_2(\cos\alpha) = P_2$. It should be also noted that the values of P_4 fall within the acceptable range, for a given P_2 value, according to the analysis of Bower[42] for uniaxially oriented polymers.

At first sight, there are two reasons for the differences in the orientability, the side chain length and the presence of the oxygen atom in the side chain that enables interchain interactions. Lateral interactions have been considered as important in aromatic polyesters containing substituted oligophenylene units in the main chain.[43] In that case, the presence of the oxygen atom as an ether linkage in the side chains resulted in the formation of various solid-state structures. This was not the case for the alkyl-substituted analogues,[44,45] which were amorphous in almost all cases.

Additional data of the PETH−Ph5/OC12.C10 polyether film with a spacer of 10 methylene units are shown in Figure 7 as well. The film of this polymer exhibits a decreased P_2 (and P_4) value, (order of 0.2 in the P_2 plateau region) that is much less than the corresponding polymer with a spacer of 11 methylene units. The reason for such a behavior might be found in a combined influence of the length of the flexible spacer and the microstructural configuration resulting from spacers with different parity in the number of methylene units. An odd−even effect[34,35] in the glass transition temperature at these materials has been previously observed, while anomalous dependence of the glass transition on the spacer length has also observed in other related systems.[46]

Lets now compare the orientability of the polyethers with the previously reported[38] results on the orientational behavior of wholly aromatic polyesters of PES−Ph3/C*n*.Ph type (depicted also in Figure 7). It is clearly shown that films with the same hexyl-type side groups, PETH−Ph5/C6.C11 and PES−Ph3/C6.Ph, exhibit comparable P_2 values (∼0.6) regardless to the presence of either aliphatic or aromatic spacers. Another interesting point concerns the orientational behavior of the polyethers with hexyloxy side chains where lower P_2 values (∼0.3) are obtained for the studied aromatic−aliphatic polyethers, contrary to the expectation that the presence of the flexible spacer would enhance the orientability of these polymers. This result denotes once more the importance of the lateral interactions on the orientational ability and the overall behavior of this type of polyether film.

The overall form of P_2 curves versus draw ratio plots in Figure 7 suggests that the orientation behavior of these aromatic−aliphatic polyethers can be represented by the affine deformation model of Kratky,[47] which gives a more rapid initial orientation. This model compares qualitatively well enough with the obtained P_2 data, and represent to a good approximation the orientation of rigid rods in a viscous matrix, suggesting that elongation rather than shear may be the dominant mechanism of orientation during the drawing deformation of most of these polyethers. The same model quantitatively compares better with the P_2 data obtained from polyether films with longer side chains and/or absence of oxygen links between the alkyl side chain and the aromatic segment and at a lesser degree with the P_2 data obtained from polyether films bearing hexyloxy side chains. The most probable explanation of this discrepancy is based on the fact that although the affine deformation model is based on noninteracting rigid rods, to a certain degree this is questioned in present polyether systems and, in particular, in those with short side chain length bearing oxygen links. However, as already pointed out in refs 26, a P_2 detailed evaluation is not truly meaningful, since it is based on principles of continuum mechanics and does not provide hints on the molecular origins of the orientation mechanism.

D. Luminescence Measurements. To further investigate the anisotropic photophysical behavior of these materials, polarized photoluminescence measurements have been conducted. Both unpolarized light and polarized light have been used for excitation. The dichroic ratios were defined and calculated as the ratio between the spectra measured with polarization of the emitted light parallel and perpendicular to the drawing direction. The integrals rather than the peak maxima of the blends have been used since they are directly related to the energy of the relevant electronic transitions.[48]

The polyether PETH−Ph5/OC12.C10 has been chosen for photoluminescent measurements since it is representative for the studied polymers with regard to the orientability deduced from the Raman measurements. As a first approach, excitation with unpolarized light has been used since this situation is more relevant from the technological point of view. The results are shown in Figure 8A for a drawing ratio of $\lambda = 3$. Surprisingly very low dichroic ratios of only about 1.3 is obtained which has to be compared to a value of 3.5 obtained by Raman spectroscopy in the corresponding *v*-VV/*v*-VH polarization combination (see also Figure 8A). To elucidate this observation, having in mind that very high dichroic ratios have been obtained from diluted solutions of similar polymers in polyolefins,[30] blends of the abovementioned polymer in polypropylene have been prepared and studied. *i*-PP has already been used as a host polymer in oriented polymer/dye polarizer films with enhanced drawability and improved performance with respect to polarized efficiency.[49] Low concentrations have been used, since the orientation of the photonic polymer is not influenced by the composition in the low concentration regime.[48] Results of the photoluminescence behavior of the blend containing 1% of PETH−Ph5/OC12.C10 in *i*PP are shown in Figure 8B at draw ratio 4. In this case, a dichroic ratio of 3.6 was obtained, while the corresponding Raman polarization ratio, *v*-VV/*v*-VH, was 7.6. We have to mention here that the Raman spectra (via the 1605 cm^{-1} scattering Raman band) as well as the photoluminescence measurements (via the absolute maxima of the emitted light) with parallel to the draw axis polarization geometry shown in Figure 8 have been normalized for a direct comparison aspect.

A possible explanation for the behavior observed in Figure 8, where in the case of pure polymer there is negligible polarized light emission although the macromolecular chains are oriented as shown by the Raman experiments, can be energy transfer. This can occur in dense systems, which contributes to lateral, in respect to the polymer orientation, light emission. Charge transport has been accepted as the reason polymers containing conjugated and flexible spacers show electroluminescence. Since charge carriers cannot travel over extended distances along the main chain, charge transport, which relies exclusively to interchain carrier transfers by hopping, has been considered.[22]

Nevertheless, fluorescence depolarization is a general phenomenon in systems with oriented chromophores.

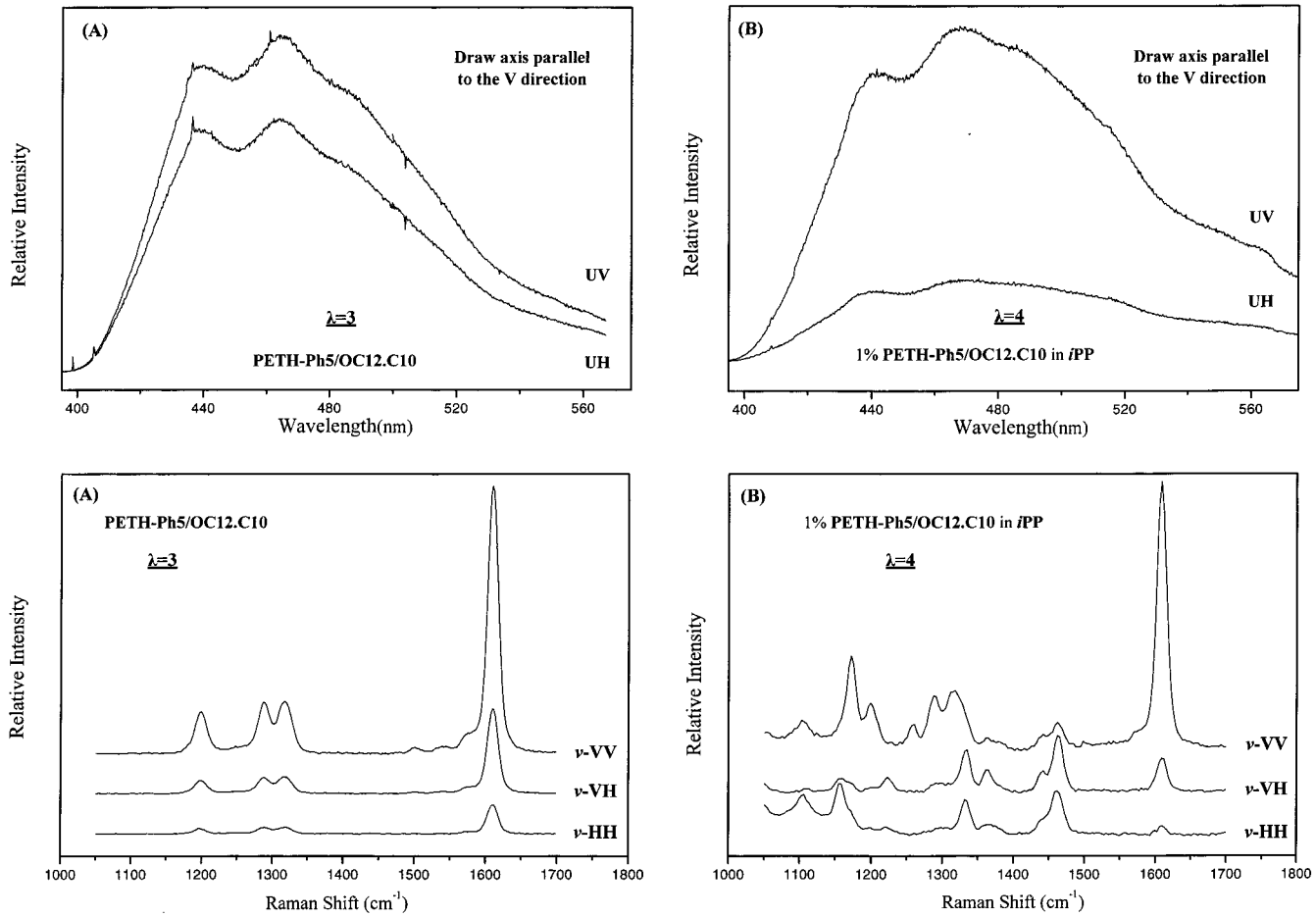

Figure 8. Polarized photoluminescent (up) and Raman (down) measurements of a drawn PETH−Ph5/OC12.C10 polyether as a homopolymer (A), $\lambda = 3$, and as a diluted blend in polypropylene (B), $\lambda = 4$. The diffused light of an UV lamp excited the photoluminescent measurements. The spectra are shifted vertically for clarity.

The reason is the migration of the excited state over all available sites modified by the orientation distribution and the lifetime of the photoexcited state (the exciton). In Raman, there are short lifetimes of picosecond order, whereas, in luminescence, there are longer lifetimes of 100 ps to 0.1 μs order. Thus, the excitation will visit many sites and, thereby, becomes randomized. This "energy transfer" needs a situation in which the chromophores are close enough to allow for excitation transfer.

In solution, the distance between most polymer chains is large enough and interchain interactions are thus minimized; this is also the case for diluted polymer blends.[50] As a consequence, the degree of polarization should increase.

Moreover, the dispersion of the active polymer in the inert matrix can be resulted either in a homogeneous mixture or in a phase-separated blend. The rigid−flexible nature of the photonic polymer might be accounted for its dispersion in terms of a phase separation in spherically shaped micelles dispersed in the matrix of the inert polymer and occupying a small fraction of the total volume.[51] To probe this model we may look into the P_2 dependence on the draw ratio, shown in Figure 6. When the draw ratio is increased, P_2 values reach a plateau. This indicates that the elongation of the dispersed particles of the active polymer is restricted by the maximum deformation that micelles undergo; subsequent drawing does not result in a further molecular alignment. This sufficient reason to prejudge a phase-separation dispersion of the active polymer is questioned by the relatively high molecular orientation of 0.7−0.9 in P_2 values attained by this polymer even at draw ratio of $\lambda = 4$ (see Figure 6). This precludes any unequivocal conclusion concerning the nature of the dispersion of the active polymer in the inert *i*-PP matrix, although the interpretation accounted for a phase separation in terms of a limited length scale defined by the size of the rigid blocks seems to be the most probable one.

The values of $\langle P_4(\cos\theta)\rangle$ shown also in Figure 6 are within acceptable limits.[42]

On the basis of the observed differences in the luminescent behavior of the pure photonic polymer and its diluted blend, they were both excited with polarized light, at various draw ratios. In the case of the pure polymer, there is no significant difference in the emission spectra regarding the polarization direction of the exciting and the emitted light even for samples drawn to $\lambda = 5$, regardless of the higher degree of orientation detected in the corresponding Raman spectra. A maximum dichroic ratio of 1.54 was obtained (see Figure 10). The same measurements have been performed in blends (1% of PETH−Ph5/OC12−C10 in PP) for various draw ratios. In Figure 9, both polarized photoluminescence (A) and polarized Raman (B) measurements of drawn films of the PETH−Ph5/OC12.C10 polyether diluted blend in polypropylene are shown. The results presented in Figure 9A show a significant improvement in the degree of polarization in the case of diluted blends, but

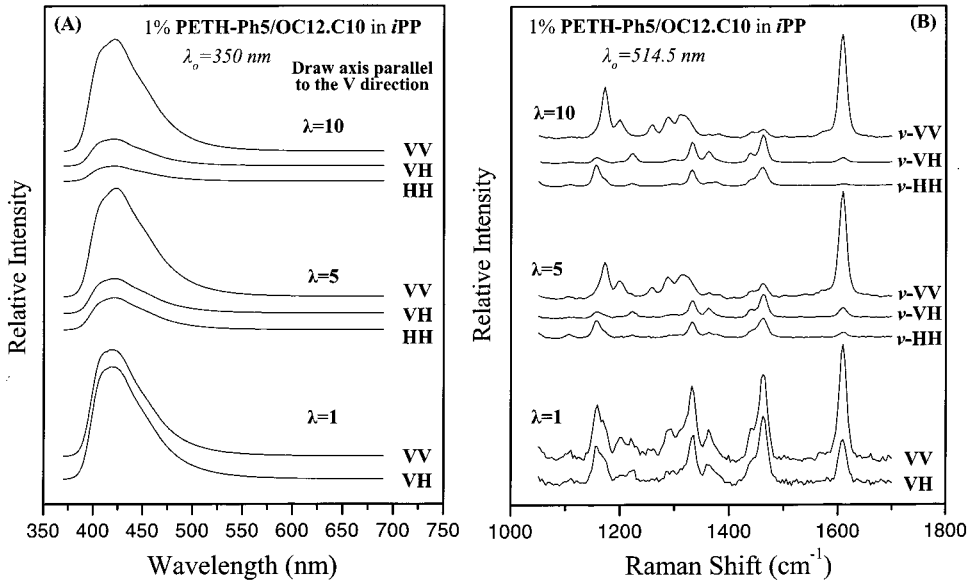

Figure 9. Polarized photoluminescent (A) and Raman (B) measurements of drawn films of the polyether, PETH−Ph5/OC12.C10, diluted blend in polypropylene. Polarized light of λ_o = 350 nm excited the photoluminescent measurements. The spectra are shifted vertically for clarity.

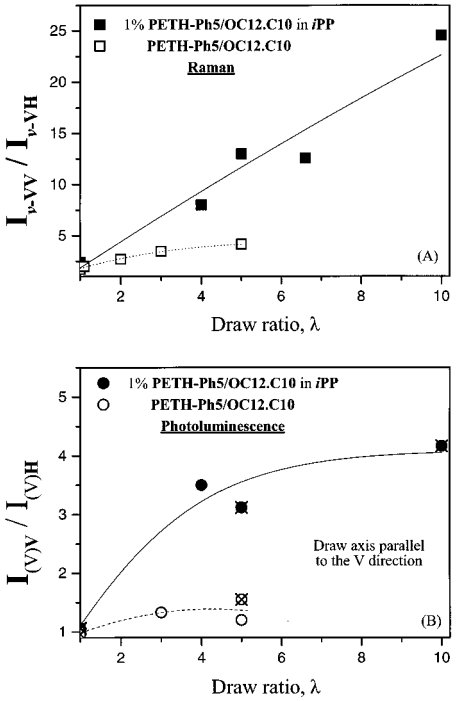

Figure 10. (A) Polarization ratio, *ν*-VV/*ν*-VH, of polyether films PETH−Ph5/OC12.C10 as homopolymer (open symbols) and as diluted blend in polypropylene (solid symbols) for the 1605 cm^{-1} phenyl ring Raman band, as a function of the draw ratio, for uniaxial drawing. (B) Dichroic ratio (measured in emission), calculated from the integrals of the respective photoluminescent spectra, as a function of the draw ratio, for PETH−Ph5/OC12.C10 films as homopolyethers (open symbols) and as diluted blends in polypropylene (solid symbols). Crossed symbols indicate photoluminescence measurements with polarized excitation light (λ_o = 350 nm) along the draw axis. Lines are drawn to guide the eye.

the obtained dichroic ratios are significantly lower than the corresponding polarization values obtained by the Raman spectroscopy (Figure 9B). By increasing the draw ratio above 5, dichroic ratio above 4 was obtained. Comparing the polarized light emission obtained from the pure photonic polymer and its dilute blend in PP, which is also shown in Figure 10B, it is clear that the dilution of the active material results also in a much higher polarization of the emitted light.

From the above discussion it is evident that there is a difference on both polarization and dichroic ratio obtained by Raman and luminescent measurements respectively when the behavior of the neat photonic material is compared with that of its diluted blend in polypropylene.

In a recent publication,[30] dealing with the photoluminescence behavior of poly(2,5-dialkoxy-*p*-phenylene−ethynylene) in ultrahigh molecular weight polyethylene, the best results, in regard to the polarized light emission, were obtained for samples containing 1−2% of the photonic material; when the concentration was increased, again good drawability was obtained but with lower dichroic ratio compared to the more dilute blends. Moreover, in a subsequent work[48] of the same photoluminescent system,[30] the dichroic ratios obtained were less than five for the draw ratio range from 10 to 20, followed by a significant increase in dichroic ratios as the draw ratios were increased up to 80.

In our case, for the PETH−Ph5/OC12.C10 polyether diluted blend in *i*-PP, dichroic ratios of 3−5 were obtained for draw ratios of 4−10. This reveals the perspective and possibility of the studied polymers to give materials with polarized blue light emission provided that an inert host−polymer with low entanglements density and very high drawability will be used.

Conclusions

We have shown that the micro-Raman technique can be effectively used for the determination of the chain configuration in oriented flexible−rigid polymers, bearing substituted quinquephenyl units in the main chain. The influence of various structural parameters such as the side chain type and length on the orientability has been examined. It has been shown that (a) the polyethers with longer side chains are more orientable and (b) the presence of the oxygen in the side chain results in interchain interactions and hence reduced orientability even compared to wholly aromatic analogues. Despite the high polarization ratio obtained by the Raman technique, for these photonic polymers very low

dichroic ratios were obtained in photoluminescent measurements. Their *i*-PP diluted blends have also been studied and materials with higher dichroic ratio have been obtained. The discrepancies observed in polarized light emission from oriented polymer films of pure photonic polyethers and their *i*-PP diluted blends have been mainly attributed to lateral interchain interactions, which may occur in dense systems.

Acknowledgment. The authors are indebted to Prof. Dr. Gerhard Wegner (MPI-P, Mainz, Germany) for helpful discussions and suggestions and to Mr. B. Zimmer (MPI-P, Mainz, Germany) for performing the polarized photoluminescent measurements. This work was partially supported by two grants (a) from the Greek General Secretariat for Research and Technology (GSRT, Oriented Research Program 1996-99, YPER-375) and (b) from the European Community (Program JOULE 1998-2000, PL-970014).

References and Notes

(1) *Developments in Oriented Polymers-1*; Ward, I. M., Ed.; Applied Science: London, 1982. *Developments in Oriented Polymers-2*; Ward, I. M., Ed.; Elsevier Applied Science: London, 1987. Ward, I. M. *Advances in Polymer Science*; Springer-Verlag: Berlin, 1985; Vol. 66, p 81. *Structure and Properties of Oriented Polymers*; Ward, I. M., Ed.; Chapman & Hall: London, 1997.
(2) Wegner, G. *Mol. Cryst. Liq. Cryst.* **1993**, *235*, 1. Ballauff, M. In *Materials Science and Technology*; Cahn, R. W., Haasen, P., Kramer E. J., Eds.; VCH: Weinheim, Germany, 1993. Ballauff, M. *Angew. Chem.* **1989**, *28*, 253.
(3) Jasse, B.; Tassin, J. F.; Monnerie, L. *Prog. Colloid Polym. Sci.* **1993**, *92*, 8. Kaito, A.; Kyotani, M.; Nakayama, K. *J. Polym. Sci., B: Polym. Phys.* **1993**, *31*, 1099.
(4) Buffeteau, T.; Desbat, B.; Besbes, S.; Nafati, M.; Bokobza, L. *Polymer* **1994**, *35*, 2538.
(5) Lafrance C−P.; Chabot, P.; Pigeon, M.; Prud'homme, R. E.; Pezolet, M. *Polymer* **1993**, *34*, 5029.
(6) Satija, S. K.; Wang, C. H. *J. Chem. Phys.* **1978**, *69*, 2739.
(7) Robinson, M. E. R.; Bower, D. I.; Maddams, M. F. *J. Polym. Sci., Polym. Phys. Ed.* **1978**, *16*, 2115; Lauchlan, L.; Rabolt, J. F. *Macromolecules* **1986**, *19*, 1049.
(8) Purvis, J.; Bower, D. I.; Ward, I. M. *Polymer* **1973**, *14*, 398.
(9) Jasse, B.; Koenig, J. L. *J. Polym. Sci. Polym. Phys. Ed.* **1978**, *16*, 2115.
(10) Li, W.; Prud'homme, R. E. *Polymer* **1994**, *35*, 3260; Abtal, E.; Prud'homme, R. E. *Polymer* **1993**, *34*, 4661.
(11) Kaito, A.; Nakayama, K.; Kyotani, M. *J. Polym. Sci., B: Polym. Phys.* **1993**, *29*, 1321.
(12) Hagler, T. W.; Pakbaz, K.; Voss, K. F.; Heeger, A. J. *Phys. Rev. B* **1991,** *44*, 8652.
(13) Dirix, Y.; Tervoort, T. A.; Bastiaansen, C. *Macromolecules* **1995**, *28*, 486.
(14) Dyreklev, P.; Bergreen, M.; Inganas, O.; Andersson, M.; Wennerstrom, O.; Hjertberg, T. *Adv. Mater.* **1995**, *7*, 43.
(15) Wittmann, J. C.; Smith, P. *Nature* **1991,** *352*, 414.
(16) Era, M.; Tsutsui, T.; Saito, S. *Appl. Phys. Lett.* **1995**, *67*, 2436.
(17) Gill, R. E.; Meetsma, A.; Hadziioannou, G. *Adv. Mater.* **1996**, *8*, 212.
(18) Gill, R. E.; Van Hutten, P. F.; Meetsma, A.; Hadziioannou, G. *Chem. Mater.* **1996**, *8*, 1341.
(19) Le Moigne, J.; Hartz, S.; Issautier, D.; Oswald, L.; Arias, E. In *Electrooptical Properties of Polymers and Related Phenomena*; Pick, R. M., Thomas, G., Bolognesi, A., Botta, C., Eds.; European Physical Society: Varenna-Paris, 1998; Vol. 22G, p IL3.
(20) Conger, B. M.; Mastrangelo, J. C.; Chen, S. H. *Macromolecules* **1997**, *30*, 4049.
(21) Lussem, G.; Festag, R.; Greiner, A.; Schmidt, L.; Unterlechner, C.; Heitz, W.; Wendorft, J. K.; Mopmeier, H.; Feldmann, J. *Adv. Mater.* **1995**, *7*, 923.
(22) Grell, M.; Bradley, D. D. C.; Inbasekaran, Woo, E. P. *Adv. Mater.* **1997**, *9*, 798.
(23) Lafrance, C.-P.; Prud'homme, R. E. *Polymer* **1994**, *35*, 3927. Gustafsson, G.; Inganas, O.; Osterholm, H.; Laakso, J. *Polymer* **1991**, *32*, 1574.
(24) Purvis, J.; Bower, D. I. *Polymer* **1974**, *15*, 645. Purvis, J.; Bower D. I. *J. Polym. Sci., Polym. Phys. Ed.* **1976**, *14*, 1461.
(25) Archer, L. A.; Fuller, G. G.; Nunnelley, L. *Polymer* **1992**, *33*, 3574. Archer L. A.; Fuller, G.G. *Macromolecules* **1994**, *27*, 4359.
(26) Voyiatzis, G.; Petekidis, G.; Vlassopoulos, D.; Kamitsos, E. I.; Bruggeman, A. *Macromolecules* **1996**, *29*, 2244.
(27) Kraft, A.; Grimsdale, A. C.; Holmes, A. B. *Angew. Chem., Int. Ed.* **1998**, *37*, 402 and references therein.
(28) Hamaguchi, M.; Yoshino, K. *Appl. Phys. Lett.* **1995**, 67, 3381.
(29) Pakbaz, K.; Heeger, A. J. *Phys. Rev. B* **1995,** *51*, 14199.
(30) Weder, C.; Sarwa, C.; Montali, A.; Bastiaansen, C.; Smith, P. *Science* **1998**, *279*, 835.
(31) Hay, M.; Klavetter, F. L. *J. Am. Chem. Soc.* **1995**, *117*, 7112.
(32) Herrema, J.K.; Van Hutten, P. F.; Gill, R. E.; Wildeman, J,; Wieringa, R. H.; Hadziioannou, G. *Macromolecules* **1995**, *28*, 8102.
(33) Kallitsis, J.; Gravalos, K.; Hilberer, A.; Hadziioannou, G. *Macromolecules* **1997**, *30*, 2989.
(34) Konstandakopoulou, F.; Gravalos, K.; Kallitsis, J. *Macromolecules* **1998**, *31*, 5264.
(35) Konstandakopoulou, F.; Kallitsis, J. *J. Polym. Sci. Pol. Chem.*, in press.
(36) Pigeon, M.; Prud'homme, R. E.; Pezolet, M. *Macromolecules* **1991**, *24*, 5687.
(37) Citra, M. J.; Chase D. B.; Ikeda, R. M.; Gardner, K. H. *Macromolecules* **1995**, *28*, 4007.
(38) Andrikopoulos, K.; Vlassopoulos, D.; Voyiatzis, G. A.; Yiannopoulos, Y.D.; Kamitsos, E. I. *Macromolecules* **1998**, *31*, 5465.
(39) Zerbi, G.; Gussoni, M.; Castiglioni, C.; In J. L. Bredas, R. Silbey Eds.; In *Conjugated Polymers: The Novel Science and Technology of Conducting and Nonlinear Optical Active Materials*; Kluwer Academic Publishers: Dordrecht, The Netherlands, 1991; p 435.
(40) Bower, D. I. *J. Polym. Sci., Polym. Phys. Ed.* **1972**, *10*, 2135.
(41) Mead, D. W. Personal communication, 1996.
(42) Bower, D. I. *J. Polym. Sci., Polym. Phys. Ed.* **1981**, *19*, 93.
(43) Kakali, F.; Kallitsis, J.; Pakula, T.; Wegner, G. *Macromolecules*, **1998,** *31*, 6190.
(44) Kallitsis, J.; Wegner, G.; Pakula, T. *Macromol. Chem.* **1992**, *193*, 1031.
(45) Kakali, F.; Kallitsis, J.; Gravalos, K. *Macromolecules* **1994**, *27*, 4509.
(46) Percec, V.; Kawasumi, M. *Macromolecules* **1991**, *24*, 6318.
(47) Kratky, O. *Kolloid Z.* **1933**, *64*, 213.
(48) Weder, C.; Sarwa, C.; Baastiaansen, C.; Smith, P. *Adv. Mater.* **1997**, *9*, 1035.
(49) Dirix, Y.; Tervoort, T. A.; Bastiaansen, C. *Macromolecules* **1997**, *30*, 2175.
(50) Kohler, A.; Gruner, J.; Friend, R. H.; Mullen, K.; Scherf, U. *Chem. Phys. Lett.* **1995**, *243*, 456.
(51) Grosberg, A. Yu, Khokhlov, A. R. In *Statistical Physics of Macromolecules*; AIP Press: Woodbury, NY, 1994; p 182.

MA9911041